



## Article

# Current Interactions Mitigation in 3-Phase PFC Modular Rectifier through Differential-Mode Choke Filter Boost Converter

José Teixeira Gonçalves <sup>1,\*</sup> , Stanimir Valtchev <sup>1,\*</sup> and Rui Melicio <sup>2,3</sup> <sup>1</sup> Departamento de Engenharia Eletrotécnica e Computador, CTS/UNINOVA, FCT, Universidade NOVA de Lisboa, 2829-516 Monte Caparica, Portugal<sup>2</sup> IDMEC, Instituto Superior Técnico, Universidade de Lisboa, Av. Rovisco Pais 1, 1049-001 Lisboa, Portugal; ruimelicio@gmail.com<sup>3</sup> ICT, Escola de Ciências e Tecnologia, Universidade de Évora, Rua Romão Ramalho 59, 7002-554 Évora, Portugal

\* Correspondence: jt.goncalves@campus.fct.unl.pt (J.T.G.); ssv@fct.unl.pt (S.V.)

**Abstract:** In this paper, a new way to mitigate the current interactions is proposed. The problem of current interactions arises when a modular three-phase (3-phase) rectifier (three single-phase modules) with boost converter for power factor correction (PFC) is used. A new differential-mode choke filter is implemented in the developed boost converter. The choke here is a specially made differential inductor in the input of the boost converter that eliminates the known current interactions. To prove the new concept, a study of the level of mitigation of the current interactions is presented. The control is operated in continuous driving mode (CCM), and the popular UC3854B circuit was used for this. The rectifier proposal is validated through a set of simulations performed on the PSIM 12.0 platform, as well as the construction of a prototype. With the results obtained, it is confirmed that the differential-mode choke filter eliminates the current interactions. It is observed that at the input of the rectifier, a sinusoidal alternating current with a low level of harmonic distortion is consumed from the grid. The sinusoidal shape of the phase current proves that a better power factor capable of meeting the international standards is obtained, and that the circuit in its initial version is operational. This proven result promises a good PFC operation, to guarantee the better quality of the electrical energy, being able to be applied in systems that require a high PFC, e.g., in battery charging, wind systems, or in aeronautics and spacecrafts.



**Citation:** Gonçalves, J.T.; Valtchev, S.; Melicio, R. Current Interactions Mitigation in 3-Phase PFC Modular Rectifier through Differential-Mode Choke Filter Boost Converter. *Appl. Sci.* **2021**, *11*, 1684. <https://doi.org/10.3390/app11041684>

Academic Editors: Radu Godina, Edris Poursmaeil and Eduardo M. G. Rodrigues

**Keywords:** three-phase rectifier; boost converter; interactions; differential-mode choke filter; wind energy; aeronautics and spacecrafts

Received: 30 December 2020

Accepted: 9 February 2021

Published: 13 February 2021

**Publisher's Note:** MDPI stays neutral with regard to jurisdictional claims in published maps and institutional affiliations.



**Copyright:** © 2021 by the authors. Licensee MDPI, Basel, Switzerland. This article is an open access article distributed under the terms and conditions of the Creative Commons Attribution (CC BY) license (<https://creativecommons.org/licenses/by/4.0/>).

## 1. Introduction

Most electrical loads use direct current (DC) electrical energy, which implies the use of a rectifier that converts alternating current (AC) electrical energy to DC, which is also known as a static rectifier. The rectifier was widely developed thanks to the emergence of semiconductor devices as diodes (1900s) and transistors (1950s) a story told already in [1]. There are several types of AC–DC converters (rectifiers) prepared for various loads. The character of the load depends on the respective need and the cost associated with the rectifier. Briefly, rectifiers are classified into two groups, bidirectional and unidirectional.

The bidirectional rectifiers are usually formed by a Graetz bridge (single-phase or three-phase) with transistors (MOSFETs, IGBTs, etc.), thus requiring a control circuit to drive the transistors. They are often used as a first stage for an AC–DC–AC converter, when after the rectifier the goal is to inject energy to the grid. As an example, some wind turbines apply this double conversion for producing the final AC power [2–4] or in aeronautical applications [5].

The unidirectional rectifiers use diodes as a switching device in most of the cases. There are other unidirectional rectifiers, implemented as switching converters, but they own the possibility to be reformatted into bidirectional ones. The diodes and thyristors are

naturally commutated by the periodic changes of the polarity of the AC supply voltage. These rectifiers are also commonly constructed as Graetz bridges of diodes, single-phase or three-phase ones. The diodes Graetz bridges are more attractive, as they are simple, robust, reliable, and low-cost rectifiers when compared to the bidirectional rectifiers or any sophisticated AC–DC switching converters. Single-phase rectifiers are used for loads that demand lower power, and some of them are coupled to a converter in order to reduce the disturbances that the rectifier can inject into the electrical network. The three-phase rectifiers, on the other hand, cause great disturbance in the electrical network, due to the large amount of power demanded by the load and its nature (usually inductive, sometimes capacitive and nonlinear loads), compromising the quality of the energy in the electrical network [1]. Therefore, in order to dimension the three-phase rectifiers, some important parameters must be analyzed, being the rectifier and the interface between the grid and the load [6]. Briefly, the following criteria are most important:

Criteria for connecting correctly the rectifier to the grid:

- Voltage level and its variation;
- Nominal frequency and its variation;
- Minimum power factor (PF) value allowed by the energy supplier;
- Harmonic distortion level that the energy supplier allows.

Criteria for connecting the rectifier to the load:

- Nominal voltage and respective operating current variation;
- Maximum allowed ripple of voltage and current;
- Accurate and reliable regulation of the current and voltage, as the load requires.

Additional criteria:

- Efficiency;
- Guarantee of reliability;
- Acceptable physical and mechanical parameters (weight, volume, temperature).

The drawback of the unidirectional diode or thyristor rectifiers is the high total harmonic distortion (THD) that it injects into the electric grid and the low total power factor (PF) value. With this, the rectifier compromises the quality of energy in the electrical network. As a way of safeguarding and control of the quality of energy in the electric grid, some standards are emerging. Examples of international standards used on energy quality are IEC61000-3-2 and IEC61000-3-4, and for the THD of the current injected into the electrical network, IEEE Std 519-2014 is used.

As a way to use the more sophisticated unidirectional rectifiers in the electric networks, some versions of them are aimed to improve the total harmonic distortion (THD). It can be seen in Figure 1 that some rectifiers are power factor correctors (PFC), keeping the THD as low as possible, complying with the established standards [7,8]. In most cases, another converter is associated with the rectifier, to control the current. There is also the possibility to associate an active power filter to the rectifier's input terminals, in order to compensate the currents generated by the rectifier, thus obtaining a good quality sinusoidal current [9,10] at the rectifier input. Some studies are focused on improving the efficiency of the active power filter and simplifying the control system, as in [10]. Other studies focus on implementing the hysteresis, called also Bang-Bang control [11].

In this case study, the modular three-phase rectifiers associated with a boost converter will be analyzed, as this combination improves the power factor (PF). This effect is achieved by shaping the input currents sinusoidally, thus guaranteeing a minimum THD at the input.

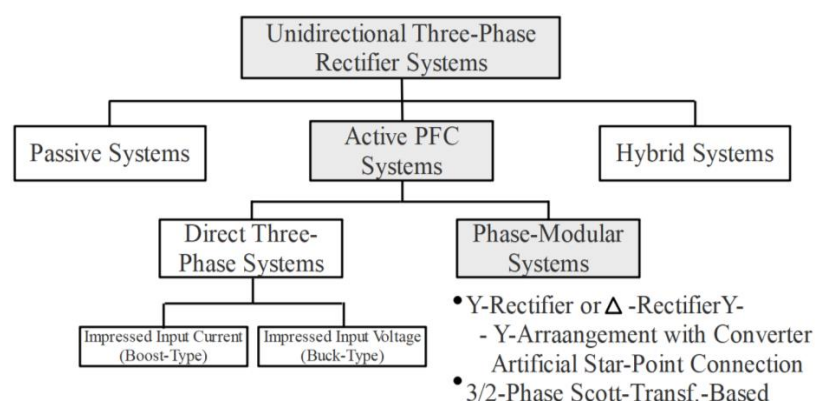


**Figure 1.** Three-phase hybrid rectifiers types [7,8].

### 1.1. Three-Phase Modular Rectifiers with Boost Converter

The three-phase modular rectifiers with additional converter are usually composed of three single-phase modules, where each module controls its phase individually. In the numerous configurations that can be created, the single-phase rectifiers interact with each other, which eliminates the possibility of control by the involved boost converter [12–14]. This becomes a problem, since the purpose of the individual rectifiers is to control the current independently and to obtain a sinusoidal current with low THD and high PF in each phase. There are some three-phase modular rectifiers that were created with the ability to eliminate those current interactions. Here, some more relevant rectifiers are suggested by this paper.

A simple way to solve the current interaction problem in a modular three-phase rectifier is analyzed in [15,16]. In this work, the author was concerned with the avoiding the interaction between the phase input currents of the rectifier. For this, a transformer is implemented at the input of each single-phase rectifier. This isolation by transformers makes the interaction current stay in the secondary circuit of each rectifier and is not seen as effect in the primary circuit. The primary currents and the sensors to control them do not see any disturbance then. In this case, the PFC is working correctly but at the expense of transformers application. The problem with this solution is that the transformers are grid frequency type, and this, depending on the power of the rectifier, obliges them to be heavy, bulky, and expensive.

In [17–19], to eliminate the current interaction, the author implemented yet another diode at the output of the negative pole of each boost converter. This diode is polarized inversely to the direction of the interaction current. An inductor at the negative terminal of the input of each boost converter do the rest of the job. The inductor of a classic boost converter in this case is split in two, one in the positive pole and one in the negative pole. The mitigation of the interaction occurs because the impedance of the inductor is high (due to the switching frequency) and therefore blocks the interaction current. Another method similar to this one but with a slight difference is presented in [20,21]. In this method, the two inductors of the boost converter are replaced by a coil winding inductor coupled to increase the inductance effect by a factor 4, as it is calculated there. By this special double-windings inductor, the filtering effect better eliminates the possible interactions. The problem of this last solution [20,21] is the increased danger of the possible saturation of the inductor, since it is a coupled inductor with concordant windings.

Another possibility is also presented in [1], where the author replaces the inductor of the boost converter with a coupled inductor of discordant windings in each converter and implements a diode at the output of the negative pole of each converter. The coupled inductor implemented in addition to the boost inductor introduces impedance differences. The impedance in the direction of the interaction current is much higher than the impedance in the direction of the normal current; thus, the circuit functions as an additional filter for the interaction current. This solution [1] shows good results. One technology problem is the winding of the inductor core, since the coupled inductor must block the passage of the

interaction current and let the normal current pass. These inductors are not easy to find ready to be supplied and require a special attention.

### 1.2. Problem and Objectives

As already seen, there are some techniques to mitigate current interactions in modular three-phase rectifiers with boost converter and PFC, some of which stand out better than others. The problem is that these techniques to mitigate current interactions have some characteristics that may be undesirable, such as the increase in volume, weight, saturation, and constructive complexity.

To solve these problems (volume, weight, saturation, and constructive complexity), it is proposed to introduce DMCF in each boost converter (between the inductor and the switching transistor) of the modular three-phase rectifier, to filter the current interactions. In the same way, isolate the supply circuit with the control circuit as much as possible using the interface circuit, but without losing simultaneous operation.

The general objective of this work is to propose a modular three-phase rectifier (three modules) with boost converters and power factor correction capable of mitigating current interactions through the DMCF. To achieve the general objective, it is essential to outline the specific objectives. Thus, the specific objectives to be achieved are as follows:

- Demonstrate that the DMCF is capable of mitigating the current interaction that appears in three-phase modular rectifiers (three modules) with boost converters and power factor correction;
- Show that the interface circuit is able to isolate the power circuit with the control circuit in order to avoid current interactions;
- Enable other researchers to replicate the proposed circuit by simulation and prove its functionality or develop improvements.

## 2. Design Proposal of the Three-Phase Modular Rectifier

### 2.1. Proposal of Three-Phase Modular Rectifier

The proposed three-phase modular rectifier is illustrated in Figure 2. It is composed of three single-phase rectifier modules, each of which is connected to a boost converter with control in the CCM. The connection of the rectifier to the grid can be made in star (Y) or delta ( $\Delta$ ) configuration. Here, in this particular case, it will be dealt with the star (Y) connection. This proposed rectifier has the purpose of rectifying a three-phase alternating current, producing a direct current with stable output voltage. A high PF and low THD is expected, thanks to the implementation of the differential-mode choke filter (DMCF) as a part of the boost converter. This DMCF can be implemented before or after the boost converter inductor.

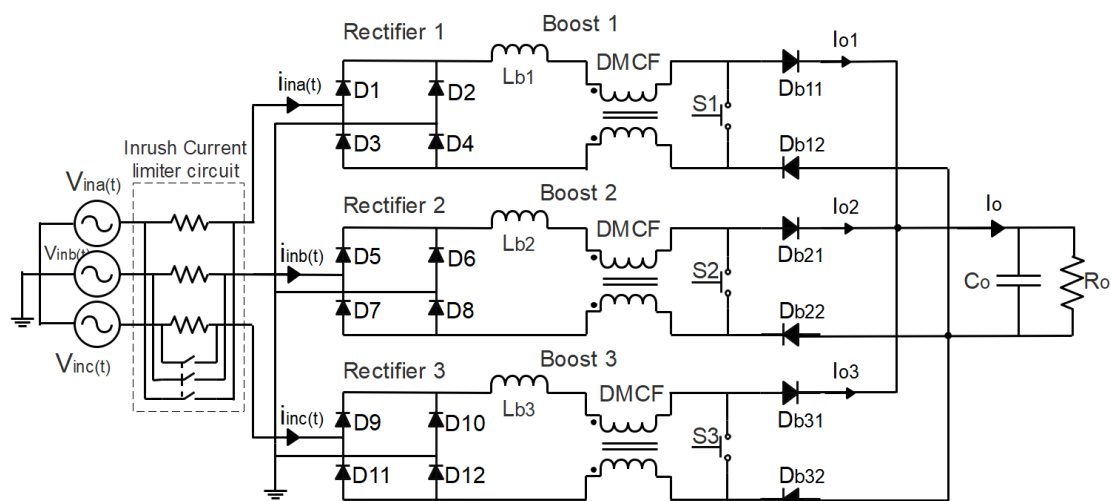


Figure 2. Proposal of three-phase modular rectifier.



## 2.2. Operating Principle of the Proposed Rectifier

This rectifier is developed precisely to work with voltage and three-phase current of sinusoidal signal, expressed by:

$$\begin{cases} V_{ina}(t) = V_p \sin(\omega t) \\ V_{inb}(t) = V_p \sin(\omega t - 120^\circ) \\ V_{inc}(t) = V_p \sin(\omega t + 120^\circ) \end{cases} \quad (1)$$

Here  $V_{ina}$ ,  $V_{inb}$ ,  $V_{inc}$  is the voltage in phase a, b, and c;  $V_p$  is the peak voltage.

The operating principle is based on Figure 2. In Figure 2, it is seen that the power supplied by the source is distributed over three paths, since the modular three-phase rectifier is composed of three rectifiers. The analysis can also be done through the input currents,  $i_{ina}$ ,  $i_{inb}$ , and  $i_{inc}$ , which will be distributed to the three rectifiers consecutively and can be calculated by:

$$\begin{cases} i_{ina}(t) = \frac{2}{3} \frac{P_o}{V_p} \sin(\omega t) \\ i_{inb}(t) = \frac{2}{3} \frac{P_o}{V_p} \sin(\omega t - 120^\circ) \\ i_{inc}(t) = \frac{2}{3} \frac{P_o}{V_p} \sin(\omega t + 120^\circ) \end{cases} \quad (2)$$

Here  $i_{ina}$ ,  $i_{inb}$ ,  $i_{inc}$  is the input current in phases a, b, and c, and  $P_o$  is the output power.

Each current will thus be rectified by its corresponding rectifier composed of a bridge of four diodes, after which a DMCF has been implemented to the respective boost converter. The DMCF and the boost stage are there in order to eliminate the current interactions (as is explained later in Section 2.3), and to serve the purpose of producing at the input of the rectifier a sinusoidal waveform of the phase current. The current is produced in phase with the voltage, thus guaranteeing a high PF and a low THD. Each rectifier connected to its boost converter thus produces an output current  $I_{o1}$ ,  $I_{o2}$ , and  $I_{o3}$ , respectively, which will then be added together, thus obtaining the output current  $I_o$  for charging the output capacitor, which acts as a filter and supplies the total current to the load. The current that charges the filter capacitor varies its amplitude, but the output voltage remains stable. As the converter is a boost converter, the output voltage will be higher than the input voltage.

The total input power can be given by:

$$P_{in} = 3 \frac{V_p I_p}{2} = V_o I_o \quad (3)$$

$$I_p = \frac{2 V_o I_o}{3 V_p} \quad (4)$$

Here,  $P_{in}$  is the input power,  $I_p$  is the peak current value,  $V_p$  is the peak voltage,  $V_o$  is the converter output voltage, and  $I_o$  is the output current.

## 2.3. Mitigation of Current Interaction

If a converter with three rectifiers and a boost converter for each rectifier is built, all connected in parallel, as in Figures 3 and 4, the interactions will appear, thus making difficult the possibility of control. For a better understanding, it will be considered an analysis in a determined angular interval of the period from  $30^\circ$  to  $90^\circ$ . Only the two most positive phases, presented in Figure 5, will be considered. It is considered that the switch of the boost converter will be in the ON or OFF condition of its switching. During the considered interval, the analysis is made by two switching states, ON and OFF.

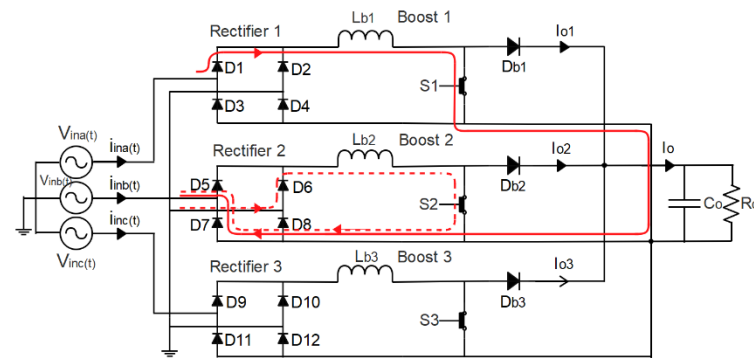


Figure 3. First interaction of current traveled in phase a.

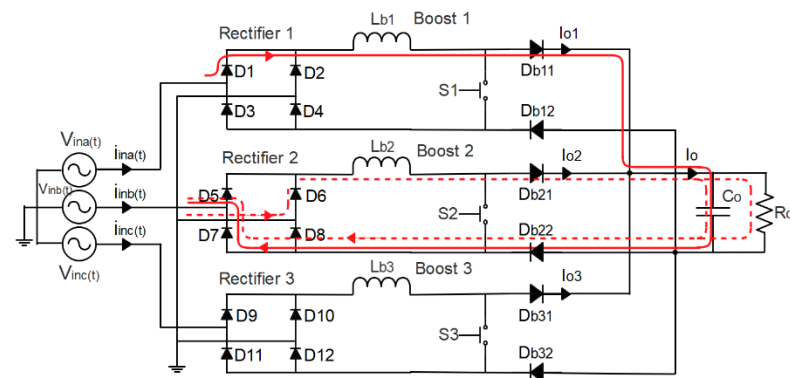


Figure 4. Second interaction of current traveled in phase a.

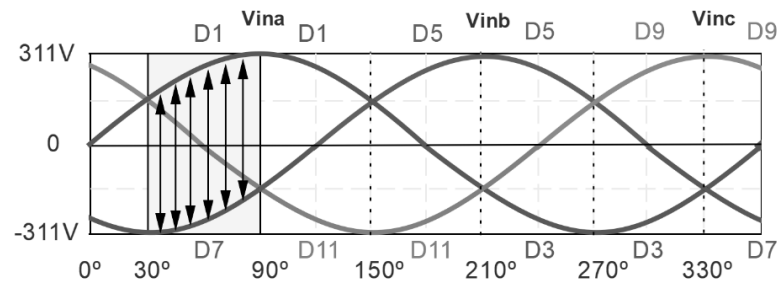


Figure 5. Interaction analysis interval.

In the ON switching state, it can be noticed that the first interaction takes place, where the interaction current will pass from diode D1 of the first rectifier and diode D7 of the second rectifier, since these diodes are directly polarized and also present a greater potential difference, that is,  $V_{ina} > 0$  and  $V_{inb} < 0$  as shown in Figure 3 [18,20,21].

In order to eliminate the ON switching interaction, a change is made in the boost converter, placing one more diode at the output of the negative terminal of each boost converter, polarized inversely to the direction of the interaction current. With this, the ON switching interaction is thus eliminated [18,20,21].

When the switching goes to the OFF state, the second interaction appears. In this second interaction, the current coming out of diode D1 will pass through the output capacitor, connecting to diode D7 of the second rectifier, since  $V_{ina} > 0$  and  $V_{inb} < 0$ , as shown in Figure 4 [18,20,21].

In order to eliminate the off switching interaction, this paper proposes the implementation of a differential-mode choke filter (DMCF) between the boost inductor and the switch, as shown in the rectifier proposed in Figure 2.

The DMCF will cause the same current that travels in the positive direction (in the primary inductor) to return in the negative direction (in the secondary inductor) of the

same phase. It is important to note that there will be no saturation in the DMCF inductors, since the core of the DMCF will cancel the magnetizing generated by the positive and negative currents, as they flow in opposite directions to the core.

The mitigation of the current interaction can be explained as follows:

As previously mentioned, and illustrated in Figure 4, the second interaction occurs because the value of the impedance where the interaction current travels (D1 to D7) is practically the same as the impedance for the normal current path (D1 to D4). Therefore, the secret is to make the impedance value for the normal current path (D1 to D4) as low as possible, in relation to the impedance value of the interaction current path (D1 to D7). This is possible when a DMCF is implemented. This change must be made in each of the three boost converters, in a way that the current of the respective boost converter travels freely along its own desired path and the path for the interaction current is made difficult.

Considering the analyzed interval of interaction (Figure 5), the circuit shown in Figure 4 can be simplified, but now including the DMCF, for a better understanding of the mitigation of the interaction. This is made in a mathematical analysis of the mitigation of the interaction current. The simplified wiring diagram is illustrated in Figure 6, where two rectifiers with their respective boost converters and the DMCF, with the normal current path ( $I_{o1}$  and  $I_{o2}$ ) and the current interaction path ( $I_t$ ), can be seen. Following this same figure, a mathematical analysis of the mitigation of the current interaction is made.

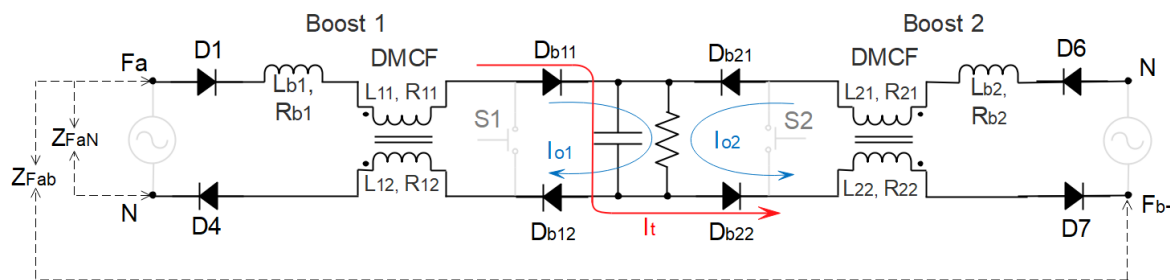


Figure 6. Representation of the analysis of current interaction mitigation in the proposed rectifier.

Here,  $F_a$  and  $F_b$  represent the phase a and b terminals,  $Z_{FaN}$  is the phase a impedance with neutral,  $Z_{Fab}$  is the impedance in the combination of the phase a with phase b,  $L_b$  is the boost inductor,  $R$  is the resistance, and  $L$  is the inductor.

#### Mathematical Analysis of Current Interaction Mitigation

Analyzing Figure 6, it is noted that the secret to a better elimination of the interaction is to make the impedance value  $Z_{FaN}$  where the normal current flows  $i_a$  are as low as possible and the value of impedance  $Z_{Fab}$  where the current interaction  $i_t$  travels is as high as possible. For this analysis, the impedances of the diodes, the output capacitor, and the load can be disregarded, since these impedances will be the same for the two analyzed paths. To do this, first the analysis of the  $Z_{FaN}$  impedance is done.

In the boost 1 converter, the currents  $I_{11}$  e  $I_{12}$  are the currents that flow through each coil of the DMCF,  $R_{11}$  and  $R_{12}$  are the two DC resistances respectively, so their impedances ( $Z$ ) are given similarly in [22]:

$$Z_1 = R_{11} + j\omega L_{11} + j\omega M \frac{I_{12}}{I_{11}} \quad (5)$$

$$Z_2 = R_{12} + j\omega L_{12} + j\omega M \frac{I_{11}}{I_{12}} \quad (6)$$

If  $L_{11} = L_{12} = L$  and  $K = 1$ , then  $M$  will be given by:

$$M = K\sqrt{L_{11}L_{12}} \quad (7)$$

Here  $M$  is the mutual inductance;  $K$  is the magnetic coupling coefficient.

Knowing that a DMCF is applied, its current travels in opposite directions in the coupled inductors ( $I_{11} = -I_{12}$ ), and if assuming that  $M = L$ , then it is obtained:

$$Z_1 = R_{11} + j\omega(L_{11} - M) \quad (8)$$

$$Z_2 = R_{12} + j\omega(L_{12} - M) \quad (9)$$

With this, it can be calculated the impedance  $Z_{FaN}$ , taking into account the impedances of the coupled inductor ( $Z_{12}$ ) and the boost inductors ( $Z_{b1}$ ), given by:

$$Z_{12} = Z_1 + Z_2 \quad (10)$$

$$Z_{b1} = R_{b1} + j\omega L_{b1} \quad (11)$$

Thus, the  $Z_{FaN}$  impedance will be given by:

$$Z_{FaN} = Z_{12} + Z_{b1} \quad (12)$$

To calculate the impedance  $Z_{Fab}$ , the path of the current  $I_t$  must first be analyzed. It is noted that it travels in three inductors connected in series ( $L_{b1}$ ,  $L_{11}$ ,  $L_{22}$ ), with  $L_{b1}$  and  $L_{11}$  being inductors in the first boost converter and  $L_{22}$  being an inductor in the second boost converter. For better understanding, the impedances will be separated in two impedances, corresponding to  $Z_{ab1}$  for the first boost converter and to  $Z_{ab2}$  for the second, as given below:

$$Z_{ab1} = R_{b1} + j\omega L_{b1} + (R_{11} + j\omega L_{11}) \quad (13)$$

$$Z_{ab2} = R_{22} + j\omega L_{22} \quad (14)$$

The  $Z_{Fab}$  impedance is given by:

$$Z_{Fab} = Z_{ab1} + Z_{ab2} \quad (15)$$

The mitigation of the current interaction occurs when the impedance  $Z_{FaN}$  is much lower than the impedance  $Z_{Fab}$ , according to (16), which proves the appearance of current  $I_a$  and not current  $I_t$ .

$$Z_{FaN} \ll Z_{Fab} \quad (16)$$

### 3. Implementation of the Proposed Three-Phase Modular Rectifier

To validate the proposed three-phase rectifier, a simulation study was carried out, using the PSIM software version 12. The construction of an experimental prototype is under development. The most important parameters used in the simulation are shown in Table 1. It is important to note that the proposed rectifier was dimensioned and analyzed for a power of 20 kW, and therefore the load has a value of 29  $\Omega$ . However, to analyze the behavior of the PF and the THD of the rectifier in changes in load resistance, it will also be evaluated for 1%, 20%, 40%, 60%, and 80% of the 20 kW power. This corresponds to loads of 289 (1%), 144 (20%), 72 (40%), 48 (60%), 36 (80%), and 29  $\Omega$  (100%).

The proposed circuit is divided (assembled) in the PSIM by three circuits, the power circuit, the interface circuit, and the control circuit, as can be analyzed in Appendix A.

**Table 1.** Parameters used in the simulation.

Components	Description	Values
$V_{lin-rms}$	RMS line voltage	380 V
F	Network frequency	50 Hz
$V_o$	Output voltage	760 V
$P_o$	Output power	20 kW
$L_b$	Inductance of boost inductor	1 mH
$L_1, L_2$	Self inductance of DMCF	1 mH
M	Mutual inductance of DMCF	0.99 mH
$C_o$	Output capacitor	3300 $\mu$ F
$R_o$	Load	29 $\Omega$
$f_s$	Switching frequency	100 kHz

Power circuit: this is where the energy is processed between the source and the load. Among the various elements constituted, the boost converter inductor, the DMCF, and the output capacitor are most important. The boost inductor  $L_b$  was calculated according to (17), whereas the output capacitor  $C_o$  is calculated by (18), similarly to the proposed in [23]:

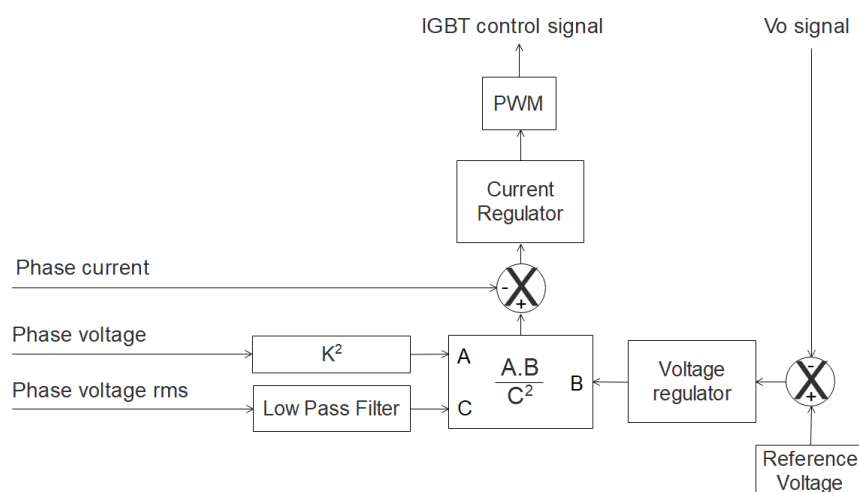
$$L_b = \frac{3 \cdot V_p^2 \cdot (2V_o - 3V_p)}{f_s \cdot \Delta I_{L\%} \cdot 4 \cdot P_o \cdot V_o} \quad (17)$$

$$C_o = \frac{2 \cdot P_o \cdot t_{hold}}{V_o^2 - (0.9 \cdot V_o)^2} \quad (18)$$

where  $f_s$  is the switching frequency,  $\Delta I_{L\%}$  is the current variation in the boost inductor in percentage, and  $t_{hold}$  is the hold-up time (the time that the system keeps the energy in the output capacitor).

The value of the inductances in DMCF, illustrated in Table 1, is chosen for a best possible operation of the circuit.

Control circuit: The control strategy for the proposed three-phase rectifier is based on [23,24]. The control technique is performed using mean values in continuous driving mode. To this end, the IC UC3854B was used, since it internally incorporates all the circuits necessary for the implementation of the control and was designed for boost converters with single-phase PFC. For better understanding, a basic diagram of the UC3854B control process is illustrated in Figure 7, in just one rectifier module. Basically, control starts at the multiplier/divider, with the reference current as the output and parameters A, B, and C as input.

**Figure 7.** Basic diagram of UC3854B control.



Parameter A is the synchronism signal, that is, a rectified sinusoid signal from the input voltage, and defines the shape, frequency, and phase of that reference signal transformed into a current signal.

Parameter B is the voltage regulator error signal, which provides control of the output voltage by varying the error signal that adjusts the amplitude of the reference current according to the load variation. It corresponds to the necessary amplitudes of the sinusoidal phase current that the rectifier should take from the input.

The parameter C is the feed-forward control signal that corresponds to the rms value of the input voltage. That signal is obtained by approximated value obtained by filtering. By this action, the reaction of the boost converter is faster, taking care for the rms variation of the input phase voltage.

In this way, the reference current depends directly on parameters A, B, and C, and is thus compared (regulated) with the current signal of the input (obtained by means of a current sensor). Then, the regulated reference current is injected into the PWM block (composed of a comparator, a sawtooth wave generator, and a control circuit) to generate the necessary control pulses for the IGBT, explained in [23].

Interface circuit: The interface circuit is responsible for making the connection between the power circuit and the control circuit in an isolated way to avoid possible interactions. In short, the isolation is done in the phase current, phase voltage,  $V_o$  signal, and the IGBT control signal.

Phase current: To obtain the current signal, a Hall effect current sensor is used, together with a precision rectifier, to rectify the sensor signal in its negative polarity half-wave, and then it is injected into the UC3854B.

Phase voltage: To obtain the voltage signal in isolation, transformers were used in each phase, with a 230 V/6 V ratio. Then, these voltages were rectified by a precision rectifier in positive polarity and sent to UC3854B. It is important to note that the signals obtained from the precision rectifier were also used by an adder to obtain the rms signal of the phase voltage.

$V_o$  signal: The isolation on this DC bus signal is more to prevent any signal or noise from the load from interfering directly in the voltage control loop. For this purpose, a Hall-type voltage sensor was used.

IGBT control signal: This is also a crucial point and must be isolated to avoid interactions. For this purpose, drivers with galvanic isolation were used in each driver canal.

### *Prototype Implementation*

The prototype is under construction (being improved and tested). The power circuit, the interface circuit, and the control circuit have already been built, as shown in Figure 8. It was built for a power of 20 kW, but the first tests are being carried out with a load of 74  $\Omega$ , which corresponds to a power of 6 kW. The values of the boost inductor, the DMCF, the output capacitor, and other technical parameters (input voltage, mains frequency, switching frequency) were constructed with values according to Table 1.

In Figure 8, (A) is the digital multimeter model IDM91E with voltage divider (1/2), with the recorded voltage value of 666 V; (B) is the digital oscilloscope model TDS3014 B of 100 MHz, and 1.25 GS/s; (C) is the boost 1 inductor, with the inductance value of 0.5 mH + 0.5 mH; (D) is the differential-mode choke filter (DMCF); (E) is control circuit 1; (F) is the circuit interface; (G) is an AC Electric Energy Tester, Model AT3010, that records the voltage value 230.8 V, the current value 9.237 A, the active power value 2.108 kW, the power factor value 0.98, the frequency value 50 Hz, and the ambient temperature value 15 °C; and (H) is the power circuit.

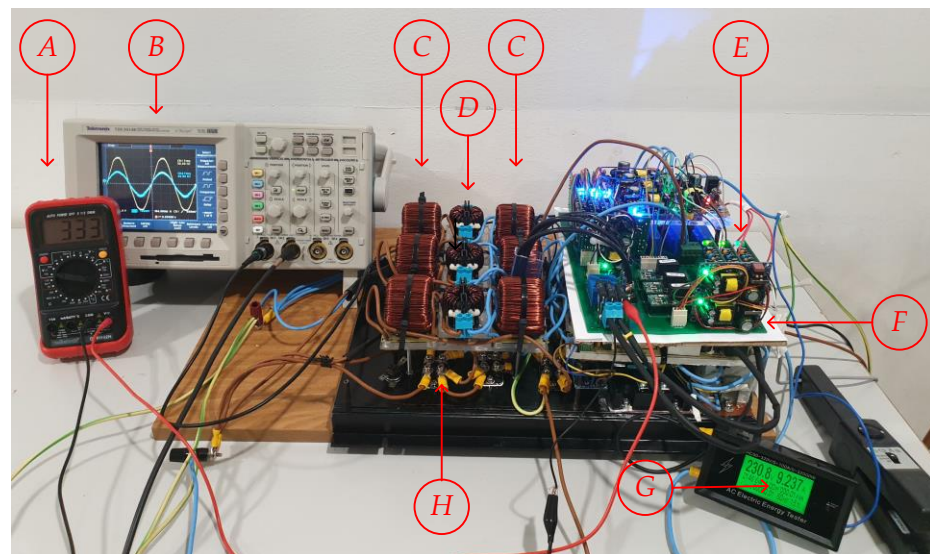


**Figure 8.** Prototype in development.

The prototype interface and control circuits are shown in Figure 9.

Figure 9 illustrates some components of the interface circuit and control circuit that are being tested due to the interconnection between them and their efficiencies. The components are: (A) is drives (CGD15SG00D2) for the correct functioning of the IGBTs (IXYN50N170CV1); (B) is the voltage hall sensor (LV 25-P); (C) is the precision rectifier; (D) is the switch control; (E) are the current hall sensors (LAH 50-P); and (F) is the control circuit 1 (UC3854B).

Some measured results from the reduced prototype tests are presented in Section 4, together with the results by simulation.

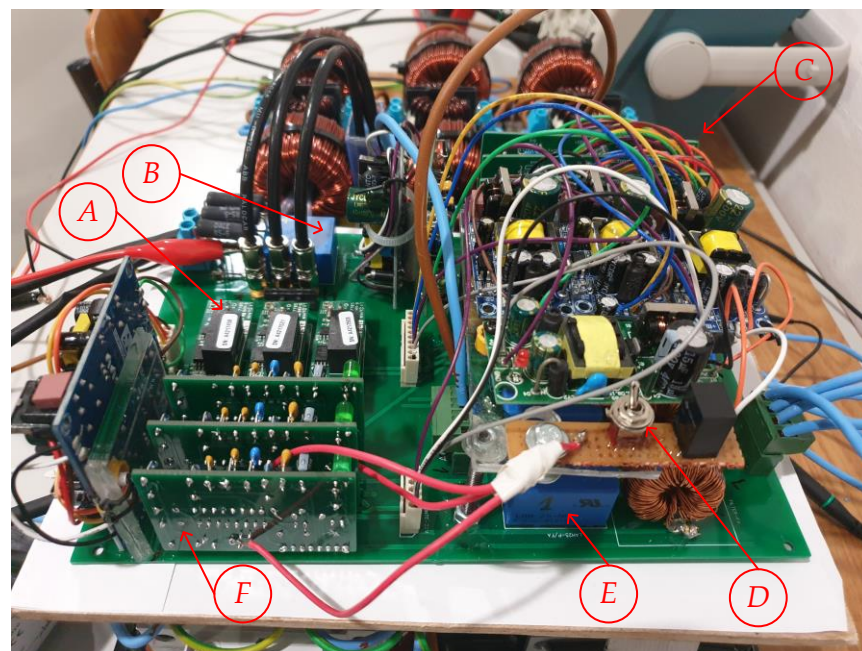


**Figure 9.** Prototype interface and control circuits.

Figure 10 illustrates the instruments used to measure current and voltage in phase a. For current measurement, a current probe on the 10 mV/A scale shown in Figure 10a was used. In the case of measuring the network voltage signal, a voltage transformer was used

for galvanically isolated measurement with a 230 V/18 V model CTFC5150-18 pro-Power ratio, illustrated in Figure 10b.



**Figure 10.** Instruments used for measurement in phase *a*: (a) current probe used in current measurement; (b) voltage transformer for galvanically isolated measurement.

#### 4. Results and Discussion

For the results obtained, the rectifier input and output parameters are analyzed. The input parameters are thus analyzed considering the values of currents, voltages, fast Fourier transform (fft) results, power factor (pf) and total harmonic distortion (thd). for the output parameters; the values of the currents and voltage are considered too. The available results of the prototype are also presented and studied.

From the input currents, the sinusoidal shape and displacement of 120 degrees between the phases is taken to prove the results. With the results, it can be concluded that the currents are being rectified by each module of the rectifier independently, and correspond to the three-phase system, as shown in Figure 11.

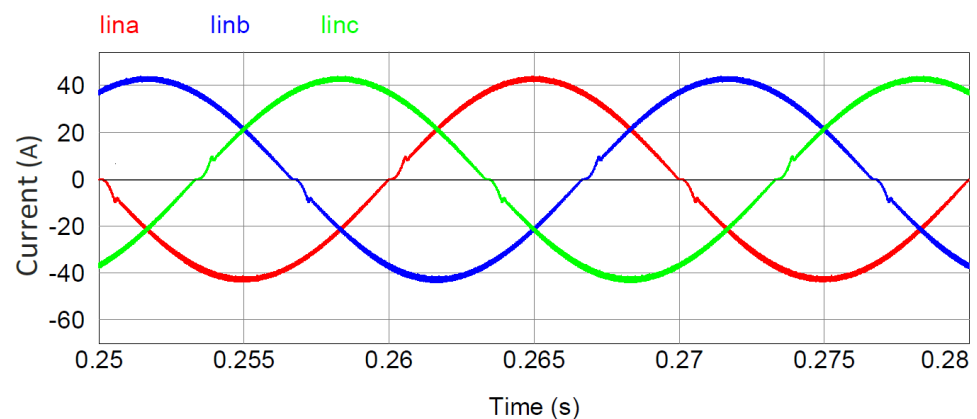


**Figure 11.** Rectifier input currents (full power, Table 1).

In order to observe the frequencies that make up the waveforms of the three currents obtained, the FFT was applied as shown in Figure 12, where it is seen that the currents are basically composed only by the fundamental frequency of 50 Hz. The resolution of the calculation could not possibly be better, and the shape near to the 50 Hz zone (1st harmonic) does not have a high precision.



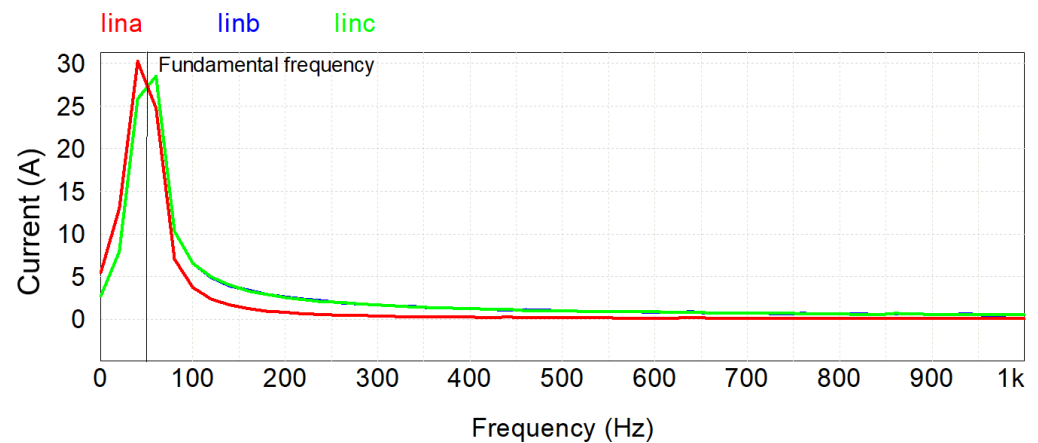


Figure 12. FFT of input currents.

The results obtained at a reduced power (roughly 2 kW per phase), from the prototype, confirm the sinusoidal shape of the phase current. The waveform of the current illustrated in Figure 13 corresponds to the current of phase *a* and was obtained by means of a current probe on the 10 mV/A scale as shown in Figure 10a; thus, the measurement on the oscilloscope as shown in Figure 13 is 10 A for each division that gives approximately 13 A peak. This peak value also corroborates with the current value of 9.2 A RMS, represented in Figure 8 (G). The waveform in Figure 11 is similar to that of the current in Figure 13, so the simulation predicts the real results well.

In this same Figure 13, it also shows an FFT analysis of the current in phase *a*. This analysis shows the fundamental frequency and some harmonics with a low value that can be also disregarded. As it is seen from Figure 13, the shape of the current was slightly asymmetrical (the voltage source was weaker), but the first harmonic is the main component of the spectrum. This analysis also corroborates with the analysis made in PSIM as shown in Figure 12.

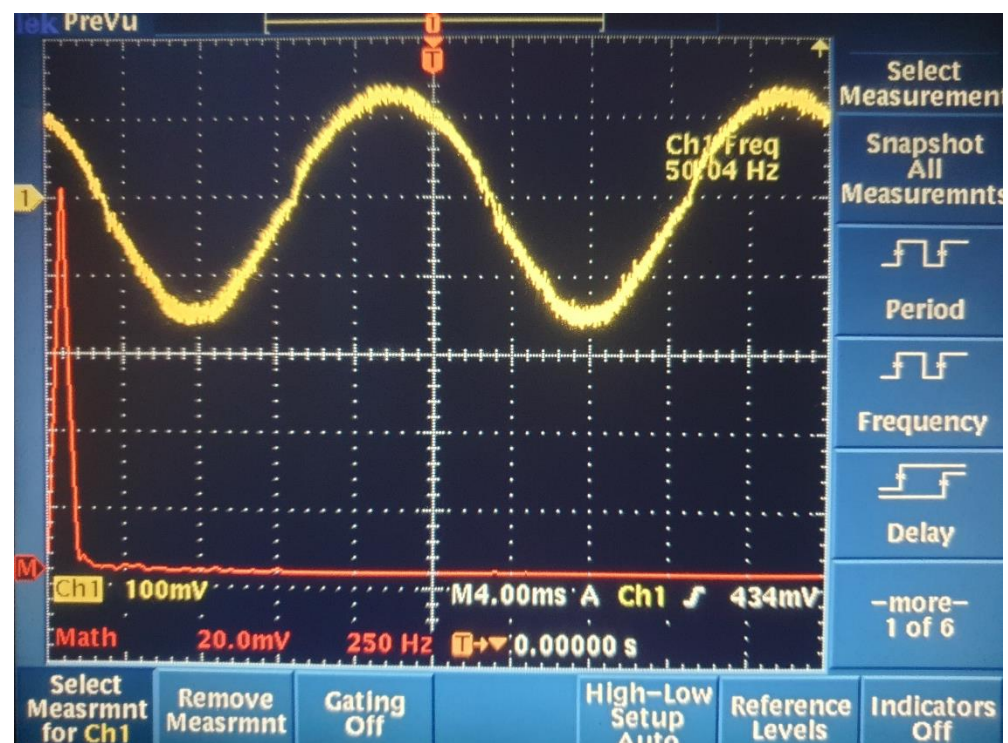


Figure 13. Waveform in phase *a* and respective FFT analysis of the prototype.

The voltage and current in phase *a* for a  $29\ \Omega$  load are shown in Figure 14, as an example for the other phases (phase *b*, phase *c*). Note that the voltage and current are sinusoidal and are in phase, which resulted in high PF and low THD.

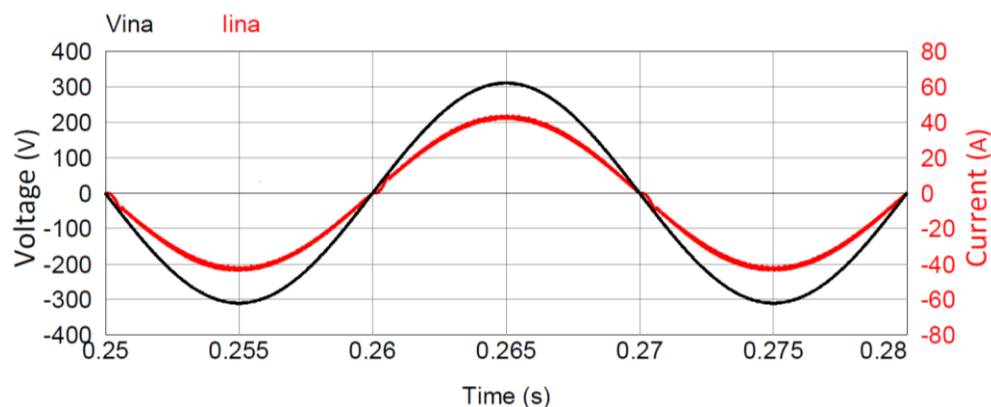


Figure 14. Voltage and currents in phase a, of the rectifier.

In order to evaluate the behavior of PF and THD more rigorously, several simulations were carried out with different levels of load as described in Section 3, which allowed obtaining Figure 15. In Figure 15a, it can be seen that the value of THD is inversely proportional to load variation, that is, as the load value increases, THD decreases, thus obtaining a maximum THD of 4.98% for a load of  $289\ \Omega$  (1%) and a minimum THD of 1.92% in load  $29\ \Omega$  (100%). The analysis of the PF illustrated in Figure 15b had the opposite behavior to THD. In this analysis, it is noted that the value of PF is directly proportional to the variation of the load, that is, as the load increases, the PF increases, thus obtaining a maximum PF of 99.98% for a load of  $29\ \Omega$  (100%) and a minimum PF of 98.13% at a load of  $289\ \Omega$  (1%).

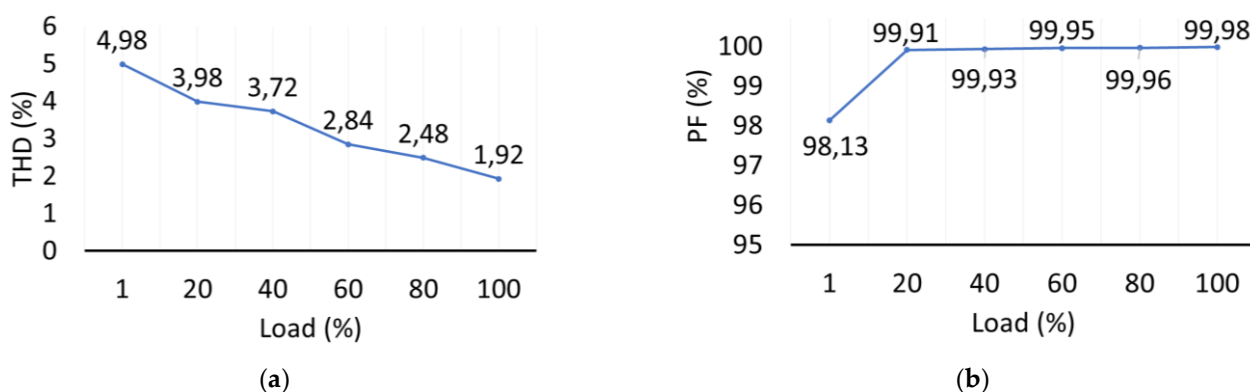


Figure 15. (a) THD for various load levels; (b) PF for various load levels.

This shows that the proposed rectifier can operate at various load levels (below the nominal load) and yet has the capacity to meet the recommendations of international standards, IEEE 519 and IEC61000-3-2/IEC61000-3-4, with regard to the quality of electricity. It is also found that the proposed rectifier is more efficient for fixed loads in which it was designed.

The voltage and current in phase *a* of the prototype is illustrated in Figure 16. The voltage form was obtained by means of a voltage transformer for galvanically isolated measurement with a 230 V/18 V ratio, shown in Figure 10b; the current was obtained by means of a current probe on the 10 mV/A scale, shown in Figure 10a. This figure shows that the current is in phase with the phase voltage, and therefore the PF value is 98% (by



the digital oscilloscope), a value very close to the value given by the simulation: 99.93%, with a load of  $72\ \Omega$  (40%). This proximity to the values also shows that the prototype is working correctly.

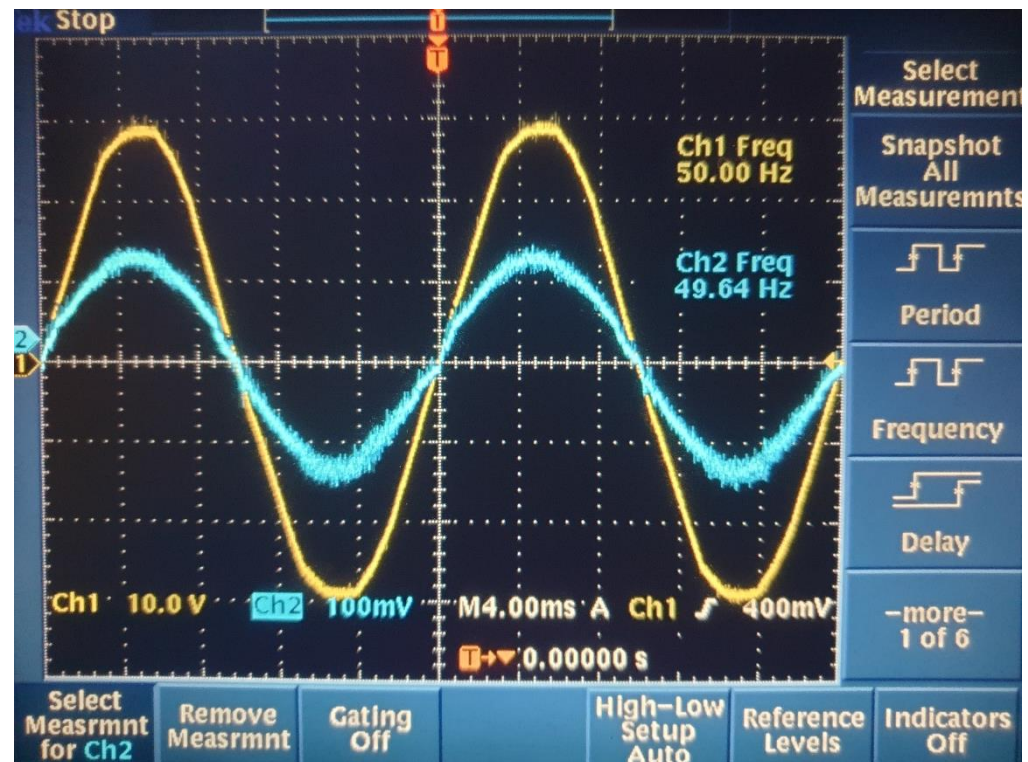


Figure 16. Voltage and current in phase *a*, of the prototype.

The starting process interval of the rectifier was analyzed, where it is seen in Figure 17 that there is a peak current transient interval of approximately 10 ms, with a maximum peak current of 200 to 700 A (inrush current). After approximately 30 ms, it is seen that the rectifier starts to operate with the PFC. The inrush current problem will be solved by applying an active method. This active method is based on the application of resistors at the input of each rectifier to limit the starting current, as shown in Figure 2. After the period of the starting current has passed, the resistors are short-circuited by means of a control and a solid-state relay. This active method to limit the inrush current has already been applied to the prototype, and it was observed that the inrush current was very low, to the point of not causing problems at the time of starting the prototype.

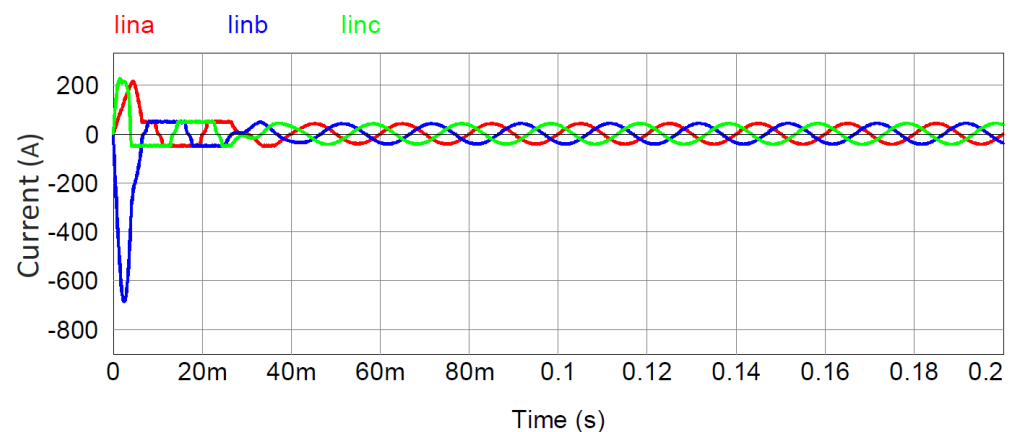
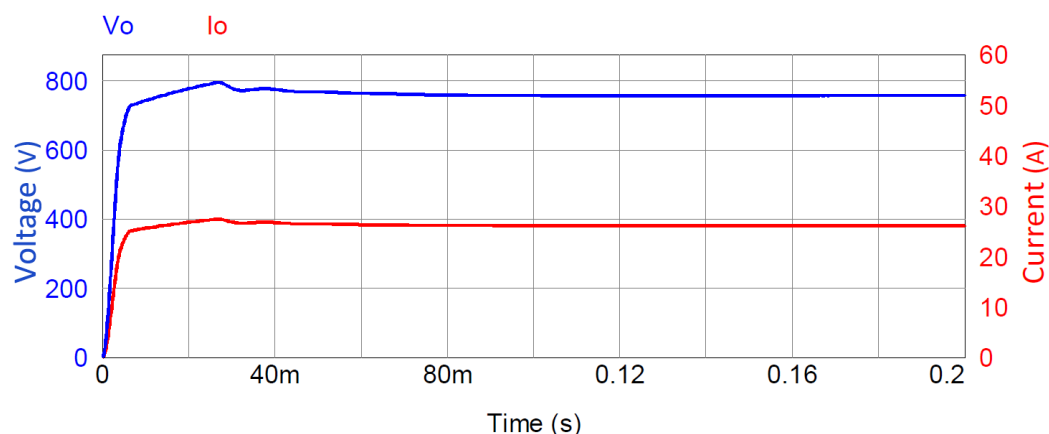


Figure 17. Analysis of the starting period of the rectifier in the three phases.

For the output variables, as seen in Figure 18, the transient interval is also similar. The voltage goes up, until it reaches a stable value of approximately 760 V in 50 ms. The output current also has a similar behavior, reaching a current of 26.2 A later. In the case of voltage and current ripple, they have a very low value that is practically negligible, which is good for many applications.



**Figure 18.** Voltage and current at the rectifier output.

Regarding the output voltage in the prototype, it still presents some difficulties. The measured value was about 666 V, as can be seen in Figure 8 (voltmeter with voltage divider  $1/2$ ), different from what was desired at 760 V. The problem is found in the control circuit of the output voltage together with the hall sensor (LV 25-P), and it is already being analyzed.

## 5. Conclusions

The construction of three-phase modular rectifiers (three modules) with boost converters and power factor correction presents a problem of current interaction, when the rectifier modules are connected in parallel and without filters at the input or output. Some techniques to avoid interactions are found in the literature, but they still have some problems such as increased volume, weight, and saturation and construction complexity. To eliminate the current interaction, it is proposed to introduce the differential-mode choke filter (DMCF) in each module of the three-phase modular rectifier in order to obtain an isolation between the phases, because the DMCF maintains the impedance value where the normal current travels and increases the impedance in the path of the current interaction.

The methodology of connecting the power circuit to the control circuit through the interface circuit seems feasible, as it allows the isolation between the two circuits (power and control).

According to the results, obtained from the proposed rectifier through simulation in PSIM and through an experimental prototype, there is shown the possibility of mitigating current interactions. This possibility guarantees the correction of the power factor value and guarantees a low total harmonic distortion that meets the recommendations of international standards. Although the prototype is still in the testing phase, the first results already obtained and presented, jointly with the results from its simulation, demonstrate the operation of the presented innovation. Thus, the proposed rectifier, with the insertion of the DMCF into the modular three-phase rectifiers with boost converter and CFP, is functional and applicable.

The results are considered preliminary and need better validation, as described below, in future works.

### Future Works

To continue the study of the modular three-phase rectifier proposed in this work, it is recommended to build a prototype and apply digital control.

**Prototype:** In this work, the results are considered preliminary, due to the simulation procedure that was used for validation and the first results of the prototype test. To improve the validation of the DMCF in a modular three-phase rectifier with boost converter, it is recommended to build 10 or 20 kW prototypes to be applied in wind systems or in aeronautics and spacecrafts.

**Digital control:** In this work, analog control was applied using the UC3854B integrated circuit. This type of control has some technical disadvantages. Since digital electronics has shown great gains in terms of application of control in converters, it is recommended to apply a digital control in the rectifier proposed. An example of integrated circuits with digital control that can be applied is the XMC1402-Q040  $\times$  0128 AA. In this way, the analog control (UC3854B) can be compared with the digital control used.

**Author Contributions:** Creation and development of the proposed circuit: J.T.G.; analysis and validation of the proposed circuit and proofreading: S.V.; analysis, validation, and proofreading: R.M. The other parameters were made by the authors in a mutual way. All authors have read and agreed to the published version of the manuscript.

**Funding:** This research received no external funding.

**Institutional Review Board Statement:** Not applicable.

**Informed Consent Statement:** Not applicable.

**Data Availability Statement:** Not applicable.

**Acknowledgments:** Portuguese Foundation for Science and Technology and CTS, project UIDB/00066/2020; Foundation for Science and Technology (FCT) under the LAETA project UIDB/50022/2020; Foundation for Science and Technology (FCT) under the ICT (Institute of Earth Sciences) project UIDB/04683/2020.

**Conflicts of Interest:** The authors declare no conflict of interest.

## Appendix A

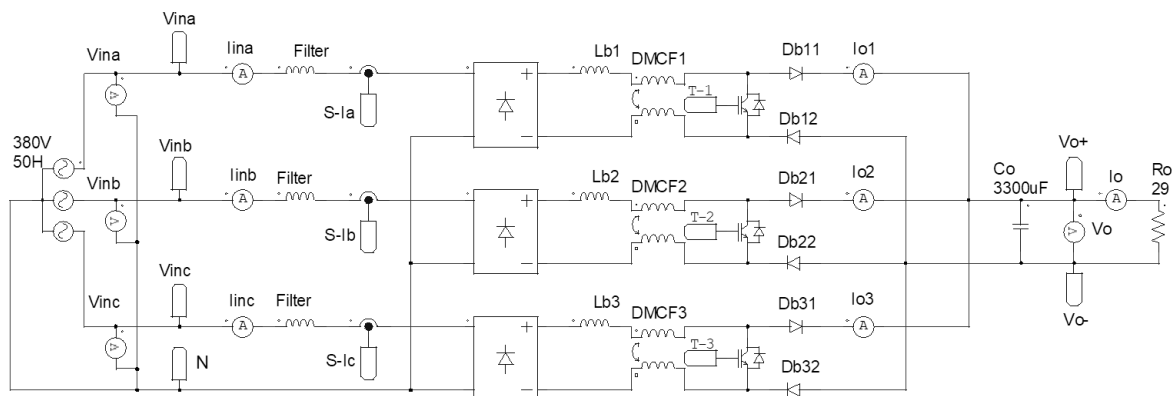


**Figure A1.** Power circuit.

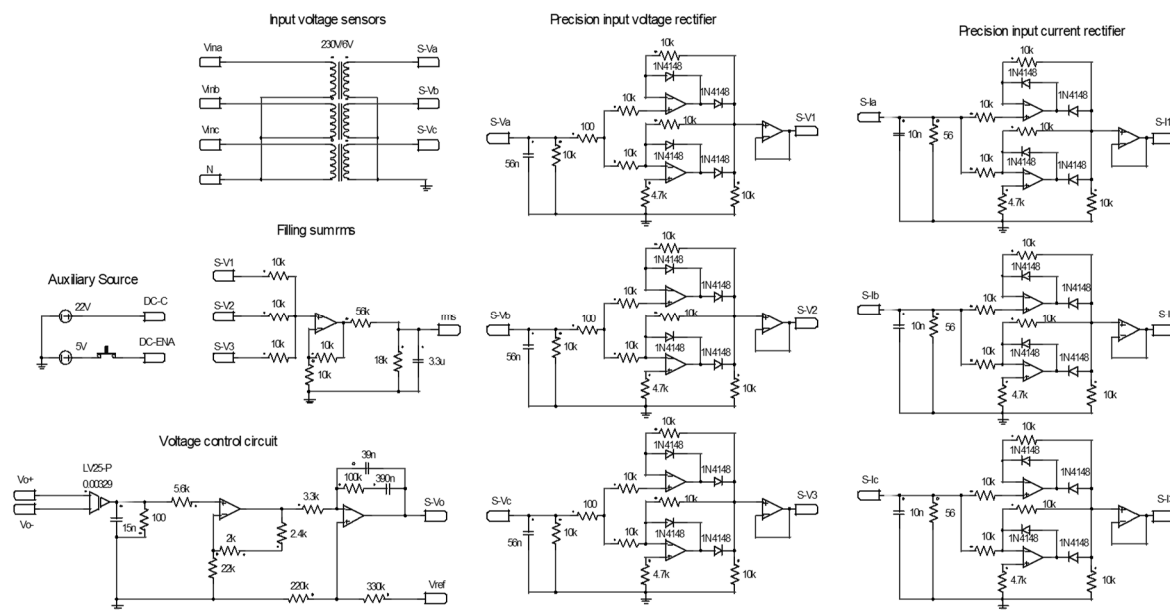


Figure A2. Interface circuit.

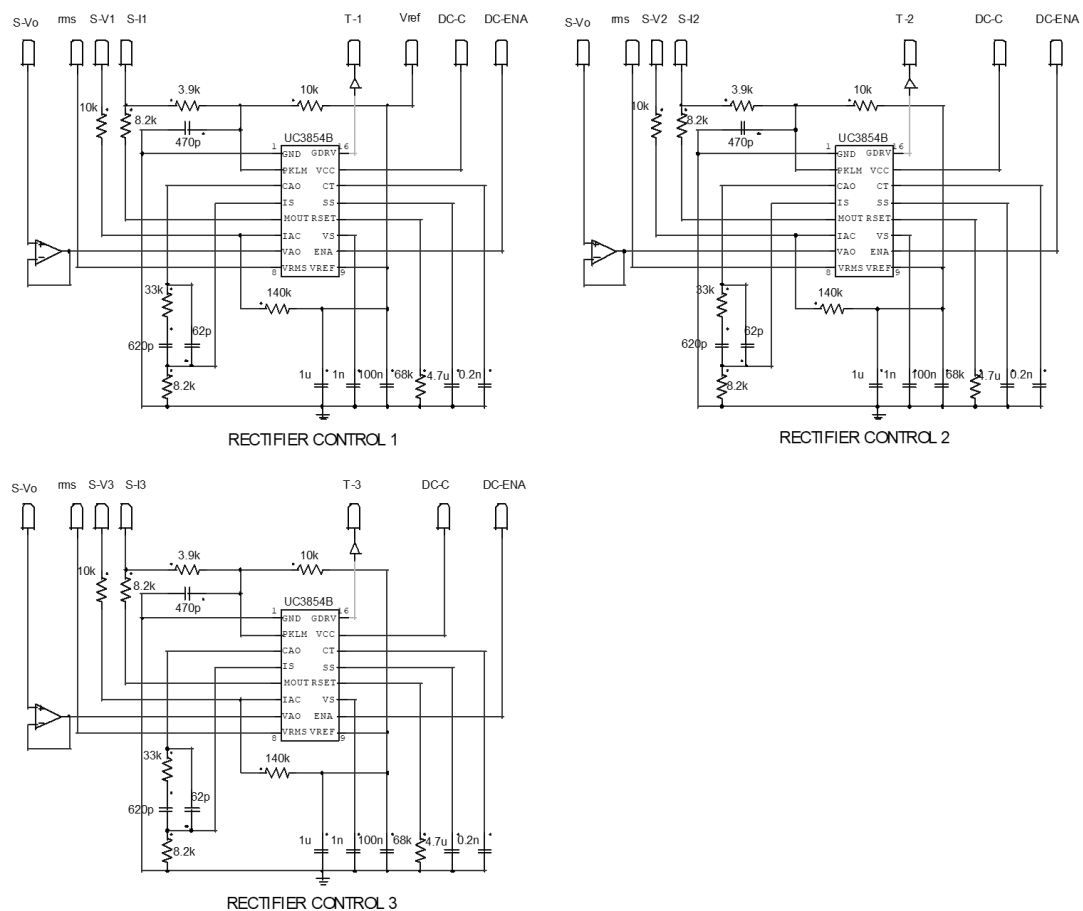


Figure A3. Control circuit.

## References

1. Gonçalves, J.T.; Valtchev, S.; Melicio, R.; Al-Saadi, M. Three-phase unidirectional transformerless hybrid rectifier with boost converter. In Proceedings of the IEEE 1st Global Power, Energy and Communication Conference (GPECOM), Nevsehir, Turkey, 12–15 June 2019; pp. 158–163.

2. Melicio, R.; Mendes, V.M.F.; Catalão, J.P.D.S. A pitch control malfunction analysis for wind turbines with permanent magnet synchronous generator and full-power converters: Proportional integral versus fractional-order controllers. *Electr. Power Compon. Syst.* **2010**, *38*, 387–406. [CrossRef]
3. Blaabjerg, F.; Liserre, M.; Ma, K. Power electronics converters for wind turbine systems. *IEEE Trans. Ind. Appl.* **2011**, *48*, 708–719. [CrossRef]
4. Seixas, M.; Melicio, R.; Mendes, V.M.F. Fifth harmonic and sag impact with a balancing new strategy for capacitor voltages. *Energy Convers. Manag.* **2014**, *79*, 721–730. [CrossRef]
5. Cavallo, A.; Guida, B.; Buonanno, A.; Sparaco, E. Smart buck-boost converter unit operations for aeronautical applications. In Proceedings of the IEEE 54th Annual Conference on Decision and Control (CDC), Osaka, Japan, 15–18 December 2015; pp. 4734–4739.
6. Siebert, A.; Troedson, A.; Ebner, S. AC to DC power conversion now and in the future. *IEEE Trans. Ind. Appl.* **2002**, *38*, 934–940. [CrossRef]
7. Kolar, J.W.; Friedli, T. The essence of three-phase PFC rectifier systems. In Proceedings of the 2011 IEEE 33rd International Telecommunications Energy Conference (INTELEC), Amsterdam, The Netherlands, 9–13 October 2011; pp. 1–27.
8. Kolar, J.W.; Hartmann, M.; Friedli, T. Three-Phase PFC Rectifier and AC-AC Converter Systems-PART 1. In Proceedings of the Tutorial at the Applied Power Electronics Conference and Exposition (APEC 2011), Fort Worth, TX, USA, 6–10 March 2011; pp. 6–10.
9. Sandeep, G.J.S.M.; Rasoolahammed, S. Importance of active filters for improvement of power quality. *IJETT* **2013**, *4*, 1164–1171.
10. Habibullin, M.; Pikalov, V.; Mescheryakov, V.; Valtchev, S. Active power filter with common dc link for compensation of harmonic distortion in power grids. In Proceedings of the 2014 16th International Power Electronics and Motion Control Conference and Exposition, Antalya, Turkey, 21–24 September 2014; pp. 1345–1349.
11. Antchev, M.H.; Petkova, M.P.; Antchev, H.M.; Gourgoulitsov, V.T.; Valtchev, S. Study of a single-phase series active power filter with hysteresis control. In Proceedings of the 11th International Conference on Electrical Power Quality and Utilisation, Lisbon, Portugal, 17–19 October 2011; pp. 1–6.
12. de Freitas, L.G.; Simões, M.G.; Canesin, C.A.; de Freitas, L.C. Programmable PFC based hybrid multipulse power rectifier for ultra clean power application. *IEEE TPEL* **2006**, *21*, 959–966. [CrossRef]
13. de Freitas, L.G.; Simoes, M.G.; Canesin, C.A.; de Freitas, L.C. A novel programmable PFC based hybrid rectifier for ultra clean power application. In Proceedings of the IEEE 35th Annual Power Electronics Specialists Conference, Aachen, Germany, 20–25 June 2004; Volume 3, pp. 2172–2177.
14. Barbosa, P.M. Three-Phase Power Factor Correction Circuits for Low-Cost Distributed Power Systems. Ph.D. Theses, The Bradley Department of Electrical and Computer Engineering, Virginia Polytechnic Institute and State University, Blacksburg, VA, USA, 2002.
15. de Freitas, L.G.; Coelho, E.A.; Simões, M.G.; Canesin, C.A.; de Freitas, L.C. Um novo retificador trifásico híbrido multipulsos com elevado fator de potência. *Eletrônica Potência*. **2005**, *10*, 17–24.
16. de Freitas, L.G.; Vincenzi, F.; Freitas, M.A.A.; Fernandes, E.R.; Mendonça, R.G.; de Freitas, L.C. Programmable PFC based hybrid multipulse power rectifier with sinusoidal input line current imposed by digital controller. In Proceedings of the APEC 07—Twenty-Second Annual IEEE Applied Power Electronics Conference and Exposition, Anaheim, CA, USA, 25 February–1 March 2007; pp. 1356–1361.
17. Mao, H.; Lee, C.Y.; Boroyevich, D.; Hiti, S. Review of high-performance three-phase power-factor correction circuits. *IEEE Trans. Ind. Electron.* **1997**, *44*, 437–446.
18. Spiazzi, G.; Lee, F.C. Implementation of single-phase boost power-factor-correction circuits in three-phase applications. *IEEE Trans. Ind. Electron.* **1997**, *44*, 365–371. [CrossRef]
19. Hahn, J.; Enjeti, P.N.; Pitel, I.J. A new three-phase power-factor correction (PFC) scheme using two single-phase PFC modules. *IEEE Trans. Ind. Appl.* **2002**, *38*, 123–130. [CrossRef]
20. Flores-Bahamonde, F.; Valderrama-Blavi, H.; Bosque, J.M.; Martínez-Salamero, L. Modular-based PFC for low power three-phase wind generator. In Proceedings of the 2011 7th International Conference-Workshop Compatibility and Power Electronics (CPE), Tallinn, Estonia, 1–3 June 2011; pp. 125–130.
21. Flores-Bahamonde, F.; Valderrama-Blavi, H.; Bosque-Moncusi, J.M.; Martinez-Salamero, L.; Leon-Masich, A.; Barrado, J.A. Single-Phase PFC for Three-Phase Wind Generator, a Modular Approach. *System* **2012**, *7*, 56–60.
22. Application Note, AN4511: Common Mode Filters, Life Augmented. Available online: [https://www.st.com/content/ccc/resource/technical/document/application\\_note/d2/4d/6f/9d/bc/80/4d/97/DM00119609.pdf/files/DM00119609.pdf/jcr:content/translations/en.DM00119609.pdf](https://www.st.com/content/ccc/resource/technical/document/application_note/d2/4d/6f/9d/bc/80/4d/97/DM00119609.pdf/files/DM00119609.pdf/jcr:content/translations/en.DM00119609.pdf) (accessed on 3 October 2020).
23. Todd, P.C. UC3854 controlled power factor correction circuit design. *UNITRODE Appl. Note* **1999**, U-134, 269–288.
24. BARBI, I. *Retificadores Monofásicos com Correção Ativa do Fator de Potência Empregando o Conversor Boost*; Santa Catarina:UFSC: Florianópolis, Brazil, 2015.